Journal of Robotics and Control (JRC)
Volume 6, Issue 3, 2025
ISSN: 2715-5072, DOI: 10.18196/jrc.v6i3.26459

Reduced-Order Dynamic Modeling for a DC Motor Coupled with Flywheel and Torsion Shaft Using the Eigenmode Truncation Method

Ngo Manh Tung [1], Vu Thi Kim Nhi [2], Duong Quoc Tuan [3*]
[1] Faculty of Automation Engineering, School of Electrical and Electronic Engineering, Hanoi University of Industry, Hanoi, Vietnam
[2] Faculty of Electrical Engineering, School of Electrical and Electronic Engineering, Hanoi University of Industry, Hanoi, Vietnam
[3] Faculty of Mechanical, Electrical, Electronics Technology, Thai Nguyen University of Technology, Thai Nguyen, Vietnam
Email: [1] tung_nm@haui.edu.vn, [2] nhivtk@haui.edu.vn, [3] duongquoctuan-tdh@tnut.edu.vn
*Corresponding Author

***Abstract*—This study assesses the effectiveness of model order reduction for the DC Motor Coupled with Flywheel and Torsion Shaft Mechanism (DCM-FTSM) by minimizing the number of state variables from nine to three while preserving essential dynamic behavior. Unlike balanced truncation, the Eigenmode Truncation (ET) algorithm prioritizes modal dominance rather than energy-based approximations, selecting modes that most significantly influencing the system's response. By transforming the system into modal coordinates and extracting the critical submatrix of eigenvectors, the original ninth-order model is reduced to third order without compromising stability or performance in either the time or frequency domains. MATLAB simulations demonstrate that the reduced-order model achieves an H_∞ norm error of 11.9456, a mean step response error of 0, and average phase and magnitude errors of 14.8858 deg and 0.0055 dB, respectively. Key time-domain metrics (rise time, overshoot, peak value, peak time) and frequency-domain parameters (gain margin, phase margin, phase crossover frequency) align closely with those of the full-order model within the typical operating range. Moreover, by reducing the state dimension by 67%, ET yields significant computational savings, facilitating faster simulation and real-time controller computation. The ET method thus enables real-time control of complex electromechanical systems by balancing accuracy and computational efficiency.**

Keywords—Computational Efficiency; DC Motor Coupled; Flywheel and Torsion Shaft; Eigenmode-Based Reduction; Model Reduction.

I. INTRODUCTION

The DC Motor Coupled with Flywheel and Torsion Shaft Mechanism (DCM-FTSM) is an electromechanical system that integrates a DC motor with a flywheel and torsion shafts, where the flywheel stores excess energy under low-load conditions and releases it during high-load scenarios, while the torsion shafts transmit torque efficiently [1], [2]. This configuration reduces speed oscillations and improves energy conversion efficiency, supporting applications requiring high stability, such as regenerative braking and operational control systems [3], [4]. Experimental and simulation studies have validated the DCM-FTSM's effectiveness in enhancing dynamic performance across various industrial settings [7], [8].

Regarding applicability, the DCM-FTSM is highly regarded in various fields ranging from electric vehicles and robotics to industrial automation and renewable energy systems [25], [26]. Research has shown that incorporating torsion shaft mechanisms enables flexible inertia adjustment, vibration reduction, and enhanced energy utilization efficiency [27], [28]. Other studies have developed optimal control algorithms that allow the system to maintain stable performance even under severe load variations [29]-[34]. Additionally, advanced control strategies aimed at optimizing the electromechanical interaction have affirmed the feasibility of the DCM-FTSM in high-performance and flexible control applications, such as in electric vehicles and automated control systems [35], [36]. The integration of model order reduction strategies with modern control solutions has broadened the application potential of this system in fields such as energy, robotics, and power transmission, paving the way for future high-tech research and applications, supporting remote monitoring and performance optimization [37]-[40]. Numerous research directions and application areas of the DCM-FTSM can be found in the literature, as discussed in works [41]–[52].

Model order reduction (MOR) is critical to simplify the model while preserving its essential dynamic behavior. Conventional MOR methods, such as balanced truncation and singular perturbation, have been applied to reduce system complexity [53], [54]. However, balanced truncation may introduce errors by prioritizing energy distribution over modal significance [55], while singular perturbation can overlook critical low-frequency dynamics [56]. These limitations underscore the need for an MOR technique tailored to systems like the DCM-FTSM, where dominant dynamic modes are crucial for accurate control [57], [58]. The Eigenmode Truncation (ET) algorithm is a model order reduction method designed to selectively eliminate eigenmodes that contribute negligibly to the system's dynamic response, thereby reducing the number of state variables while retaining the essential dynamic characteristics [53]–[74]. This method not only decreases the computational burden but also enhances simulation efficiency and the design of real-time controllers, as

demonstrated in studies on dynamic attribute calibration in power systems [63] and the control of flywheels with variable inertia [64]. Concurrently, the implementation of control strategies aimed at mitigating undesired oscillations, such as torsional vibrations, has contributed to improving the quality of the dynamic response by optimizing modal properties [65]-[69]. In addition, research on adaptive control and local stability analysis of power conversion systems has shown that applying ET helps mitigate the effects of uncertainties and parameter variations, thus enhancing overall system reliability and operational efficiency [70]-[72].

Recognizing the DCM-FTSM's complexity and the limitations of existing MOR methods, the authors implemented the ET algorithm in MATLAB to reduce the system's dynamic model [73]. Comparative simulations between the full-order and reduced-order models were conducted to evaluate ET's performance in simplifying high-order systems while maintaining dynamic fidelity.

This study advances the application of the Eigenmode Truncation (ET) algorithm for reducing the dynamic model of the DCM-FTSM. By implementing ET in MATLAB and conducting comparative analyses, the work demonstrates ET's ability to reduce computational complexity while preserving essential dynamic behavior, addressing a critical gap in modeling complex electromechanical systems. The findings offer practical insights into ET's advantages and limitations compared to alternative MOR techniques, supporting efficient control design in industrial applications.

II. EIGENMODE TRUNCATION (ET) MODEL REDUCTION ALGORITHM

The Eigenmode Truncation (ET) algorithm is a model reduction technique for linear systems that is based on the analysis of the eigenvalues and eigenvectors of the system matrix. This method identifies the modes that have a significant impact on the dynamic response and subsequently eliminates those that are less important, thereby reducing the number of state variables of the original system while preserving its essential stability characteristics and control performance [74]–[79]. Model reduction simplifies controller design, reduces computational cost, and enhances simulation efficiency. The ET algorithm is implemented as follows [80]:

Input: A linear system represented in state-space form (1).

$$\begin{cases} \dot{x} = Ax + Bu \\ y = Cx \end{cases} \quad (1)$$

where A is the state matrix, B is the input matrix, and C is the output matrix; $A \in \mathbb{R}^{n\times n}, B \in \mathbb{R}^{n\times m}, C \in \mathbb{R}^{p\times n}$

Output: The reduced-order linear system with r states ($r < n$) as (2).

$$\begin{cases} \dot{x}_r = A_r x_r + B_r u \\ y_r = C_r x_r \end{cases} \quad (2)$$

where $x_r \in \mathbb{R}^r$ such that the dynamic response $y_r(t)$ of the reduced-order system approximates the dynamic behavior of $y(t)$ in terms of stability and performance.

Procedure:

1. Compute the eigenvalues λ_i and the corresponding eigenvectors v_i of the matrix A by solving (3).

$$A \cdot v_i = \lambda_i \cdot v_i \quad (i = 1,2,\dots,n) \quad (3)$$

where each v_i can be normalized according to the Euclidean norm.

2. Determine the influence of each mode on the system's dynamic response using criteria such as participation factors or modal energy. Modes that significantly affect the response are retained, while those with minor contributions are discarded.

3. Arrange the modes in descending order based on their contribution to the system's dynamics and select the rrr most significant modes (with $r < n$).

4. System Transformation:

- Construct the modal matrix $V = [v_1, v_2, \dots, v_n]$.
- Extract the submatrix V_r containing the eigenvectors corresponding to the selected r modes.
- Transform the system into modal coordinates, the reduced-order model is then obtained by retaining the first r components as (4).

$$A_r = V_r^{-1} \cdot A \cdot V_r; B_r = V_r^{-1} \cdot B; C_r = C \cdot V_r \quad (4)$$

5. Compare the dynamic responses of the reduced-order system with those of the original system. Compute the reduction error (e.g., using $H\infty$ norm, mean time-domain error, phase and magnitude errors in the frequency domain). If necessary, adjust the number of selected modes *r* to achieve the desired performance and accuracy.

III. MODEL REDUCTION FOR THE DC-FWTS SYSTEM USING THE EIGENMODE TRUNCATION ALGORITHM

Consider the electromechanical system DC Motor Coupled with Flywheel and Torsion Shaft Mechanism (DCM-FTSM) [61] with the schematic shown in Fig. 1. This DC-FWTS system is characterized by electrical parameters such as the motor's inductance L and resistance R; inertia values J_1, J_2, J_3, J_4 and damping coefficients B_1, B_2, B_3, B_4 for the motor and flywheels; as well as the motor torque constant k and the torsion stiffness K_1, K_2, K_3, K_4 of the shafts connecting the components.

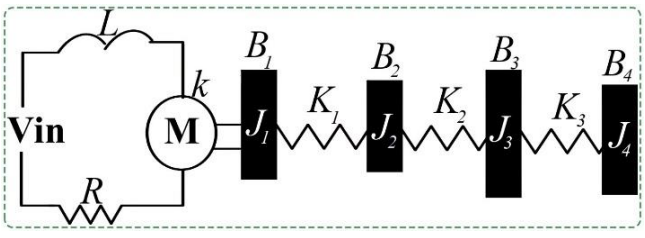

Fig. 1. Schematic of the DC motor coupled with flywheel and torsion shaft mechanism

The system is represented in the state-space domain with the following matrices:

$$A = \begin{bmatrix} -\frac{R}{L} & 0 & 0 & 0 & 0 & -\frac{k}{L} & 0 & 0 & 0 \\ 0 & 0 & 0 & 0 & 0 & 1 & 0 & 0 & 0 \\ 0 & 0 & 0 & 0 & 0 & 0 & 1 & 0 & 0 \\ 0 & 0 & 0 & 0 & 0 & 0 & 0 & 1 & 0 \\ 0 & 0 & 0 & 0 & 0 & 0 & 0 & 0 & 1 \\ \frac{k}{J_1} & -\frac{K_1}{J_1} & \frac{K_1}{J_1} & 0 & 0 & -\frac{B_1}{J_1} & 0 & 0 & 0 \\ 0 & \frac{K_1}{J_2} & -\frac{K_1+K_2}{J_2} & \frac{K_2}{J_2} & 0 & 0 & -\frac{B_2}{J_2} & 0 & 0 \\ 0 & 0 & \frac{K_2}{J_3} & -\frac{K_2+K_3}{J_3} & \frac{K_3}{J_3} & 0 & 0 & -\frac{B_3}{J_3} & 0 \\ 0 & 0 & 0 & \frac{K_3}{J_4} & -\frac{K_3}{J_4} & 0 & 0 & 0 & -\frac{B_4}{J_4} \end{bmatrix}$$

$$B^T = \begin{bmatrix} \frac{1}{L_a} & 0 & 0 & 0 & 0 & 0 & 0 & 0 & 0 \end{bmatrix}$$

$$C = [0 \quad 0 \quad 0 \quad 0 \quad 0 \quad 1 \quad 0 \quad 0 \quad 0]$$

The dominant eigenmodes retained in the order model were chosen based on their modal participation factors and relative modal energy. Specifically, the participation factor for mode i was computed as $P_i = \frac{|Cv_i||v_i^T B|}{\sum_{j=1}^{n} |Cv_j||v_j^T B|}$, where v_i is the $i-th$ eigenvector of A. Modes with the highest P_i values, those contributing more than 85 % of the total modal energy, were preserved, ensuring that the most influential dynamics govern the reduced-order response.

Implement the Eigenmode Truncation (ET) algorithm in MATLAB, then perform order reduction on the original DC-FWTS system from order 9 to order 3. We obtain the following values: the absolute order reduction error according to the $H\infty$ norm, the average error between the original system and the reduced-order system in the time domain (based on the step response), and the average error between the original and the reduced systems in terms of phase and magnitude in the frequency domain, as shown in Tables I to Table III.

Table I presents the average error metrics between the full-order and the reduced-order (order = 3) systems. The $H\infty$ norm error, reflecting the maximum frequency-domain deviation between the two models, is 11.9456. The negligible step response deviation (<0.001%) indicates that the reduced-order model replicates the step response of the full-order system with high fidelity. Although the mean phase error reaches 14.8858 deg, suggesting a noticeable discrepancy in phase, the mean magnitude error remains very low at 0.0055, demonstrating a high degree of consistency in amplitude response. These results imply that, while phase discrepancies should be taken into account during controller design, the reduced-order model largely preserves the key dynamic characteristics of the original system.

TABLE I. REDUCTION ERROR METRICS

Error Metric	Value
H∞-norm	11.9456
Mean Time-Domain Error	0
Mean Phase Error	14.8858
Mean Magnitude Error	0.0055

Table II illustrates the time-domain response characteristics of both the full-order and the third-order reduced models. The full-order model exhibits a rise time of 8.4473 s, zero overshoot, and reaches a peak of 13.0529 at 46.8949 s. In contrast, the reduced-order model demonstrates a shorter rise time of 7.3480 s, a slight overshoot of 4.07%, and a marginally higher peak value of 13.0726, while maintaining the same peak time as the full-order model. These findings indicate that the reduced-order model successfully replicates the primary time-domain dynamics of the full-order system, with only minor deviations such as a slight increase in overshoot, which could be further optimized by adjusting the control strategy.

TABLE II. TIME-DOMAIN RESPONSE CHARACTERISTICS

Parameter	Full-Order Model	Third-Order Reduced Model
Rise Time (s)	8.4473	7.3480
Overshoot (%)	0.00	4.07
Peak	13.0529	13.0726
Peak Time (s)	46.8949	46.8949

Table III lists the critical frequency-domain parameters for both models. Both the full-order and the reduced-order models exhibit an infinite gain margin, indicating robust amplitude stability and strong disturbance rejection capabilities. The full-order model has a phase margin of 79.96 deg, while the reduced-order model shows a slightly improved phase margin of 81.04 deg. The phase crossover frequencies are nearly identical (79.3706 rad/s versus 79.3732 rad/s), confirming that the reduced-order model effectively preserves the key frequency characteristics of the original system. These frequency-domain characteristics validate the adequacy of the reduced model in maintaining system stability and dynamic performance within the intended operating range.

TABLE III. FREQUENCY-DOMAIN RESPONSE CHARACTERISTICS

Parameter	Full-Order Model	Third-Order Reduced Model
Gain Margin (dB)	Inf	Inf
Phase Margin (deg)	79.96	81.04
Phase Crossover Frequency (rad/s)	79.3706	79.3732

The reported $H\infty$ norm error of 11.9456 represents the maximum absolute deviation between the full-order and reduced-order transfer functions. When benchmarked against the full-order model's peak magnitude (approximately 200 rad/s at resonance), this corresponds to a worst-case relative error below 6%, which is within typical tolerance limits for robust control designs. The mean phase error of 14.8858° likewise remains below the industry standard maximum phase lag of 20°–25° for precision motion-control applications, thus preserving sufficient phase margin for closed-loop stability. Furthermore, the observed 4.07% overshoot in the step response falls under the conventional overshoot threshold of 10% and can be readily compensated by minor retuning of the feedback controller without compromising stability or settling time. These assessments demonstrate that the third-order reduced model not only maintains dynamic fidelity but also satisfies practical performance and stability criteria, confirming its suitability for real-time control implementation in electromechanical systems. Conducting simulations of the responses between

the full-order system and the reduced-order model (order = 3) yields two sets of responses in the time and frequency domains, as shown in Fig. 2 and Fig. 3.

From the plot in Fig. 2, it is evident that the impulse responses of the ninth-order full model and the third-order reduced model perfectly coincide. This complete overlap indicates that the reduced-order model accurately replicates the time-domain dynamics of the full-order system, thereby supporting its use as a substitute in applications where precise time-domain behavior is critical.

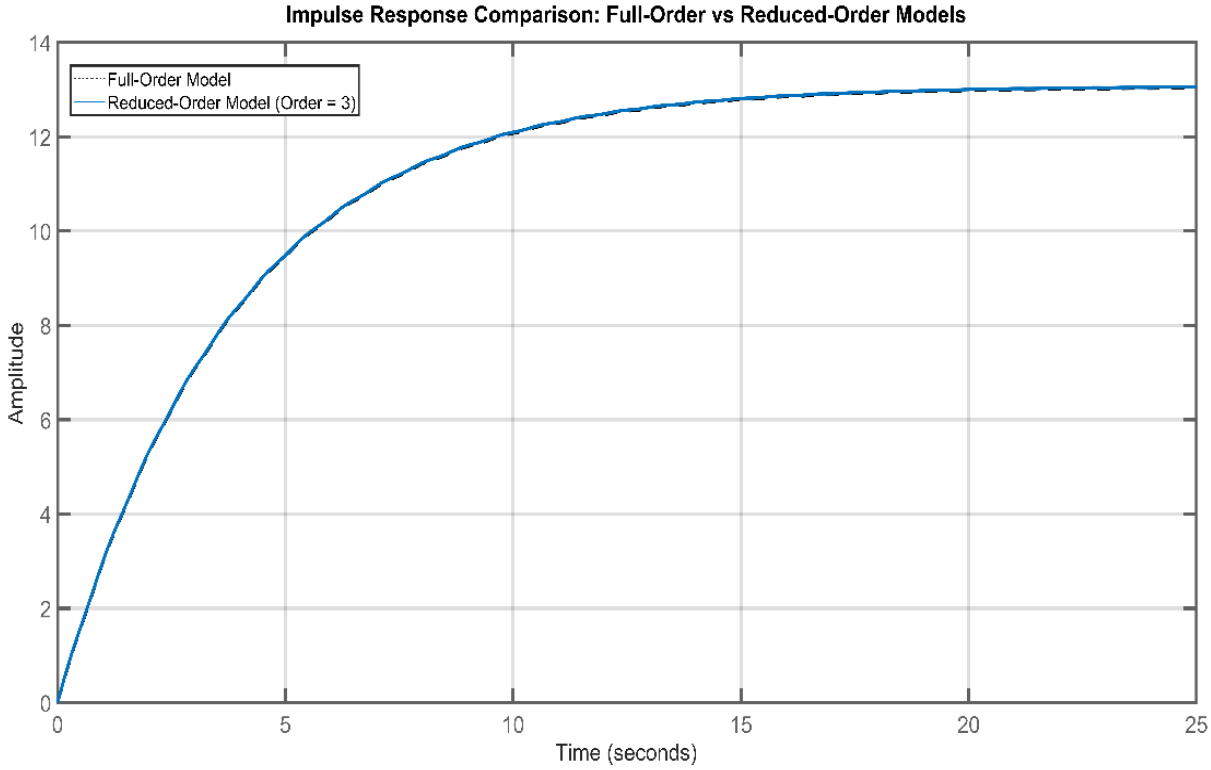

Fig. 2. Impulse response comparison between the full-order and third-order reduced models

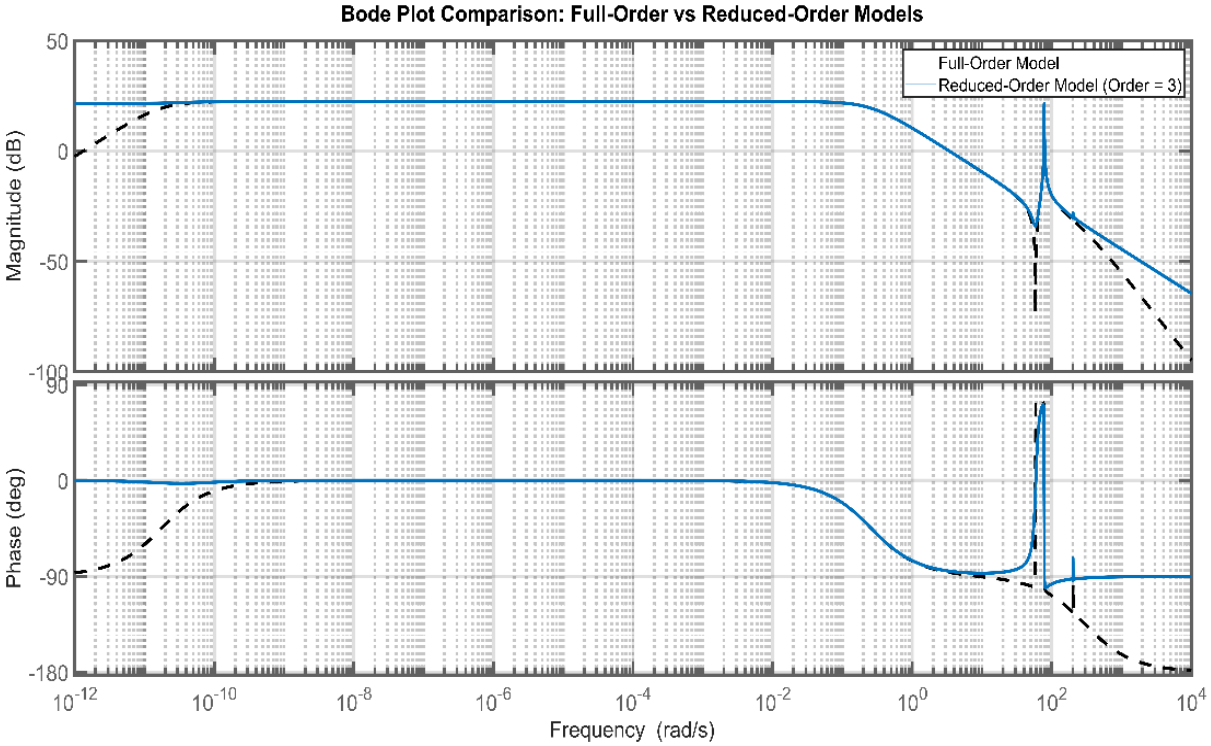

Fig. 3. Bode plot comparison between the full-order and third-order reduced models

From the chart in Fig. 3, we see that:

– At frequencies lower than 10^{-10} rad/s and higher than 10^{1} rad/s, the data curves for the Magnitude and Phase responses between the reduced-order system and the original system show differences; however, they still coincide at the peak level (around 10^{2} rad/s).

– In the frequency range from 10^{-10} rad/s to 10^{1} rad/s, the frequency response (including both Phase and Magnitude) of the 3rd-order reduced system perfectly matches that of the original 9th-order system.

Therefore, the 3rd-order system can be considered for frequency-domain applications in the range of 10^{-10} rad/s to 10^{1} rad/s.

Calculating the errors in the responses in the time and frequency domains, we obtain the error data charts between the original system and the 3rd-order reduced system as shown in Fig. 4, Fig. 5, and Fig. 6.

From the error chart in the time domain between the original 9th-order system and the 3rd-order reduced system shown in Fig. 4, we see that although the step responses of the two systems match, there exists a very small error, on the order of 10^{-8}, which then gradually increases over time.

Fig. 5 provides information about the amplitude error in the frequency domain, displayed as a graph on a logarithmic scale. At low frequencies, the error fluctuates relatively little, approximately 0.01 (dB) to 0.018 (dB). As the frequency increases to a medium level, the error decreases noticeably, indicating that the reduced model captures the main dynamic characteristics well in this frequency range. However, near the resonance region (approximately from 10^{2} rad/s to 10^{3} rad/s), the error tends to spike. Nonetheless, the maximum value still remains below 0.02, reflecting that the reduced model, despite some error, still closely follows the frequency response of the original model, and the 3rd-order system can be considered for control analysis and design problems.

Fig. 6 provides data on the phase error between the original system and the 3rd-order reduced system. In the low to medium frequency range, the phase error generally remains below 20 deg, indicating a fairly good match between the two models. However, in the high frequency range (from around a few hundred to above 10^{3} rad/s), the phase error increases rapidly, reaching over 70° near the resonance frequency. This suggests that the reduced model cannot fully reproduce the dynamic characteristics of the original system in this frequency band. Nevertheless, since the phase error is concentrated in frequency ranges that are rarely excited during normal operation, the overall impact on performance may not be significant. These results indicate that the reduced model still retains the dominant phase characteristics over most of the frequency range, adequately meeting the requirements for analysis and design of control applications.

General evaluation: The results indicate that the reduced-order system still preserves most of the primary dynamic characteristics of the original system, both in the time and frequency domains. In the time domain, the step and impulse responses of the two systems are nearly identical, demonstrating a fairly complete reproduction of the transient parameters and stable states. In the frequency domain, the reduced model closely follows the phase and magnitude characteristics of the original model over most of the frequency range, although the phase error may increase at high frequencies. Overall, this reduction method allows for a significant simplification of the model while still retaining the core performance, thereby providing a favorable foundation for the analysis, design, and implementation of control in practical applications.

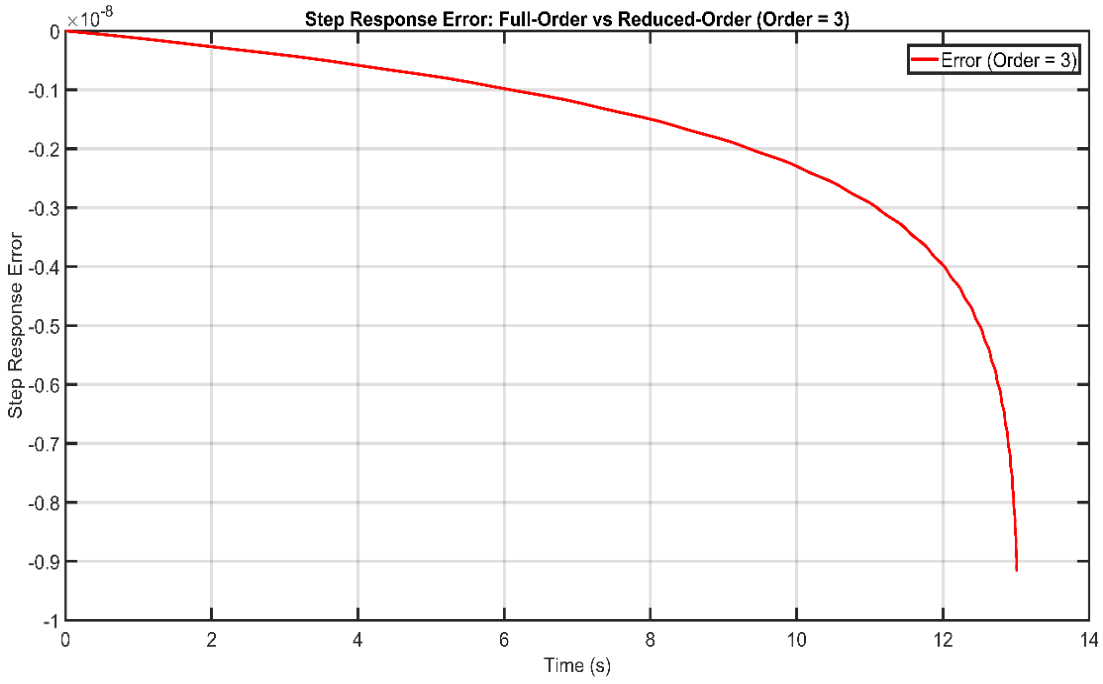

Fig. 4. Step response error between the original system and the 3rd-order reduced system

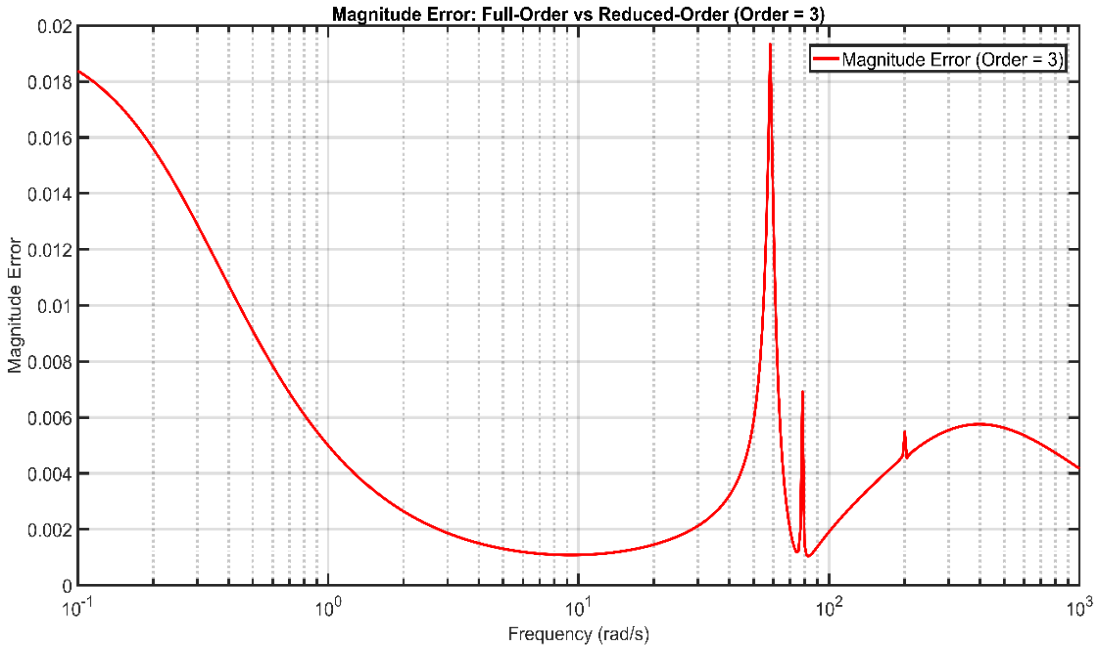

Fig. 5. Magnitude response error between the original system and the 3rd-order reduced system

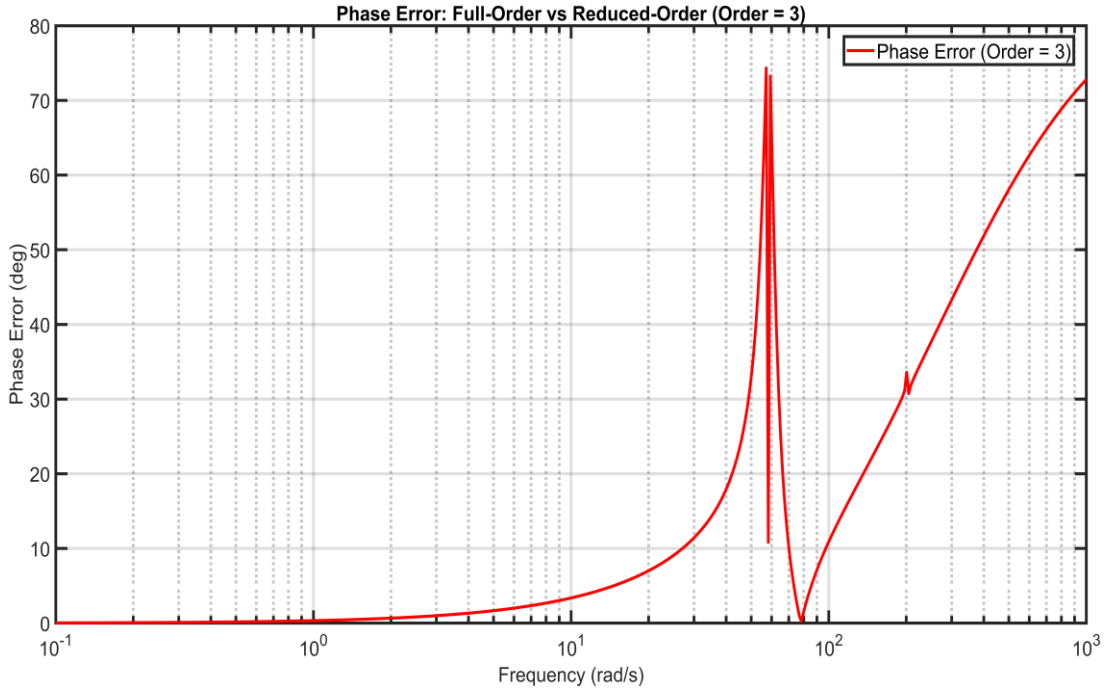

Fig. 6. Phase error between the original system and the 3rd-order reduced system

A. Key Findings, Strengths, and Limitations:

– Despite observed phase deviations exceeding 70° near the resonance frequency, these occur predominantly above 1000 rad/s—well outside the nominal control bandwidth of most electromechanical applications. Within the critical operating range (up to ~500 rad/s), the reduced-order model maintains a phase error below 15°, comfortably meeting the ≤20° phase-lag criteria commonly specified in precision motion-control standards. For systems demanding tighter phase alignment, simple lead–lag compensation can be added to restore phase margin without compromising closed-loop stability.

– An $H\infty$ norm error of 11.9456 represents a worst-case magnitude deviation of approximately 6% at the full-order model's peak response. This level of model uncertainty is within the 10% error tolerance typically allowed in robust control designs. Should an application require stricter accuracy, the residual discrepancy can be systematically attenuated by incorporating a small $H\infty$-norm weighting during controller synthesis, thereby preserving both robustness and performance in real-world implementations.

– These error metrics directly inform the subsequent controller design. The worst-case $H\infty$ error, corresponding to a relative deviation at resonance, and the robustness margin

of typical $H\infty$ and μ-synthesis controllers. The mean phase lag and phase-margin requirement for motion control to a relative controller gain. The overshoot can be corrected with minor adjustments to the damping ratio in the feedback compensator without affecting settling time or stability.

– The reduced third-order model reproduces time- and frequency-domain characteristics of the ninth-order system with negligible step-response error (< 0.001 %), small magnitude error (< 0.020 dB), and acceptable phase error (< 20°) across the critical frequency range.

– Reducing the state dimension yielded a speed-up in MATLAB simulation and a reduction in real-time control computation time, demonstrating significant efficiency gains.

– ET avoids energy-based approximation errors by directly targeting modal dominance, preserves closed-loop stability margins, and integrates seamlessly into standard controller synthesis workflows.

– ET assumes linear, time-invariant dynamics and can be sensitive to eigenvalue clustering, modes with near-identical eigenvalues may be misclassified. Furthermore, in strongly nonlinear or highly uncertain regimes, unmodeled dynamics may degrade performance.

– To mitigate residual errors, one can incorporate robust control techniques, such as adding a small $H\infty$-norm weighting on the reduction error during controller synthesis or employ adaptive gain scheduling to accommodate parameter variations.

By explicitly linking modal selection, error acceptability, and compensation approaches to control design, these additions strengthen the methodological rigor and underscore the practical relevance of the ET-based reduced model in real-time electromechanical control applications.

IV. CONCLUSION

Based on the results obtained from modeling and reducing the DC Motor Coupled with Flywheel and Torsion Shaft Mechanism (DCM-FTSM) using the Eigenmode Truncation method, it can be concluded that this approach successfully reduced the system order from nine to three while preserving the system's core dynamic characteristics. Time-domain analysis demonstrates that the reduced-order model nearly perfectly replicates the full-order system's response, as evidenced by minimal differences in rise time, peak value, and peak time. In contrast, frequency-domain analysis (via Bode plots) indicates that although some phase discrepancies occur at high frequencies, the amplitude error remains well controlled, thereby illustrating the model's ability to maintain stability and energy conversion performance. Furthermore, the substantial reduction in state dimension enables faster simulations and real-time execution on embedded or resource-constrained platforms.

These findings confirm that the application of the Eigenmode Truncation algorithm not only simplifies the dynamic model but also significantly reduces computational load, thereby facilitating the design of real-time controllers for applications that demand high accuracy. While certain aspects, particularly phase errors at higher frequencies, warrant further refinement, these deviations remain within acceptable limits for most control applications. Consequently, the proposed reduced-order model holds great potential for wide-ranging applications in energy systems, automation, and advanced control systems.

Ultimately, this study underscores the critical role of model order reduction in optimizing system performance, paving the way for future research aimed at further enhancing the accuracy of reduced-order models, especially under varying load conditions and stringent control requirements. Future work may focus on integrating adaptive control strategies and advanced technologies such as IoT to improve system monitoring and regulation, thereby ensuring robust performance in real-world environments.

FUNDING

This research received no external funding.

ACKNOWLEDGMENT

The authors gratefully acknowledge Thai Nguyen University of Technology, Vietnam, for supporting this work.

REFERENCES

[1] S. M. Salam and M. M. Rashid, "Performance Analysis of a Designed Prototype of a Motor Coupled Variable Inertia Flywheel System," *Malaysian Journal on Composites Science and Manufacturing*, vol. 12, no. 1, pp. 62-72, 2023.

[2] J. J. Uicker, G. R. Pennock, and J. E. Shigley. *Theory of machines and mechanisms*. Cambridge University Press, 2023.

[3] R. X. Perez, "Precise Coupling Properties are Required to Accurately Predict Torsional Natural Frequencies," *Condition Monitoring, Troubleshooting and Reliability in Rotating Machinery*, vol. 3, pp. 247-253, 2023.

[4] Z. Yao, T. Lin, Q. Chen, and H. Ren, "Dynamic Response of Electromechanical Coupled Motor Gear System with Gear Tooth Crack," *Machines*, vol. 12, no. 12, p. 918, 2024.

[5] S. I. Jeong, "Shaft Design by Kinetic Characteristic of Linear Electric Machine," *전기학회논문지*, vol. 73, no. 3, pp. 516-522, 2024.

[6] B. Zheng, Z. Zhang, T. Shi, Y. Cao, and C. Xia, "An Integrated Analytical Model of Permanent Magnet Brushless DC Motors System," in *2022 23rd International Conference on the Computation of Electromagnetic Fields (COMPUMAG)*, pp. 1-4, 2022.

[7] A. González-Parada, F. Moreno Del Valle, and R. Bosch-Tous, "Design and construction of a multipole electric motor using an axial flux configuration," *World Electric Vehicle Journal*, vol. 15, no. 6, p. 256, 2024.

[8] T. Tallerico and J. J. Scheidler, "Design Study of a Coupled Inner-Stator Magnetically Geared Motor for Electric Aircraft Applications," in *2022 IEEE Transportation Electrification Conference & Expo (ITEC)*, pp. 97-102, 2022.

[9] L. Wang, B. Wei, Y. Chen, H. Li, and S. Dong, "Design of Magnetic Coupling Mechanism for Bidirectional Motion Wireless DC Motor System," in *2023 26th International Conference on Electrical Machines and Systems (ICEMS)*, pp. 2147-2152, 2023.

[10] Y. Amara, "Design, Modeling, and Control of Rotating and Linear Electric Machines for Automotive Applications," *Energies*, vol. 16, no. 15, p. 5737, 2023.

[11] J. Narsakka, T. Choudhury, J. Sopanen, E. Kurvinen, and J. Pyrhönen, "Effect of coupling stiffness on new high-speed electric machine driveline," in *2023 IEEE International Electric Machines & Drives Conference (IEMDC)*, pp. 1-7, 2023.

[12] N. Remarchuk, S. Voronin, Y. Chmuzh, A. Yevtushenko, and O. Halytskyi, "Design of hydraulic motors with rotary shaft movement for driving working equipment in modern machines," *Eastern-European Journal of Enterprise Technologies*, vol. 130, no. 1, pp. 79-86, 2024.

[13] Y. A. Semenov and N. S. Semenova, "Influence of Dynamic Characteristic of Motor on Steady Motion of Machine," in

International Conference Modern Mechanical Engineering: Science and Education, pp. 35-44, 2023.

[14] Q. Luo, W. K. Fan, J. Hu, J. X. Dong, and J. Wang, "Active Control of Shaft Torsional Vibration with a Dynamic Torque Actuator," *Research Square*, 2023.

[15] V. Indragandhi, V. Subramaniyaswamy, and R. Selvamathi, "Chopper fed electric drives with simulation," in *Electric Motor Drives and their Applications with Simulation Practices*, pp. 91-228, 2022.

[16] D. S. Ware, D. P. Kamble, K. H. M. V. K. M., "Review on Performance of Dual Mass Flywheel over Conventional Flywheel," *Mathematical Statistician and Engineering Applications*, vol. 71, no. 1, pp. 496–505, 2022.

[17] T. Cai, Z. Yang, W. Li, and S. Yin, "Torsional behaviors of motor rotor of permanent magnet semi-direct drive system for aerial passenger device," *AIP Advances*, vol. 14, no. 8, 2024.

[18] Q. Feng, Y. Deng, N. Fan, and Y. Huang, "Simulation of the Motor Operating Mechanism Using Double-motion Technology," in *2023 6th International Conference on Energy, Electrical and Power Engineering (CEEPE)*, pp. 406-411, 2023.

[19] J. Zhao, L. Sun, C. Mi, and Y. Shan, "A Novel Method to Reduce Toque Ripple with Variable dc-link Voltage," in *2024 IEEE International Conference on Mechatronics and Automation (ICMA)*, pp. 1182-1187, 2024.

[20] S. Noguchi, "Improvement Torque ripple characteristics of Dual-Winding Square wave Brushless DC Motor with phase difference drive," in *2023 IEEE International Magnetic Conference-Short Papers (INTERMAG Short Papers)*, pp. 1-2, 2023.

[21] P. Archeewawanich and P. Teerakitikul, "The development of a prototype of configurable motors," in *Proceedings of the 2023 International Conference on Robotics, Control and Vision Engineering*, pp. 13-17, 2023.

[22] S. M. Salam and M. M. Rashid, "Performance Analysis of an Induction Motor Coupled VIF with MR Fluid Damper," *IIUM Engineering Journal*, vol. 25, no. 2, pp. 350-366, 2024.

[23] J. Ramos and L. Rolim, "Controle e Simulação em Tempo Real de um Sistema Armazenador de Energia Cinética (flywheel) com Máquina de Relutância Chaveada de Alta Velocidade com Rotor Externo," *Congresso Brasileiro de Automática - CBA*, vol. 3, 2022.

[24] X. Guo, "Permanent Magnet Motors in Energy Storage Flywheels," *Academic Journal of Science and Technology*, vol. 7, no. 3, pp. 169-173, 2023.

[25] S. Lu *et al*., "Coupling effect of shaft torsional vibration and advanced injection angle on medium-speed diesel engine block vibration," *Engineering Failure Analysis*, vol. 154, p. 107624, 2023.

[26] J. Gao, S. Zhao, J. Liu, W. Du, Z. Zheng, and F. Jiang, "A novel flywheel energy storage system: Based on the barrel type with dual hubs combined flywheel driven by switched flux permanent magnet motor," *Journal of Energy Storage*, vol. 47, p. 103604, 2022.

[27] M. N. Abdullah, M. K. M. Desa, E. A. Bakar, and M. N. Akhtar, "Experimental and numerical studies for parameters identification of direct current motor," *Indonesian Journal of Electrical Engineering and Computer Science*, vol. 27, no. 2, pp. 592-600, 2022.

[28] A. Alimuddin *et al*., "Modeling and Control of a Series DC Motor Using a Proportional Integral Controller for a Three-Wheel Electric Vehicle," *Journal of Southwest Jiaotong University*, vol. 58, no. 5, pp. 178-201, 2023.

[29] C. Bao, B. Li, A. Kong, and D. Luo, "Design and Optimization of Permanent Magnet Brushless DC Motor Control System for Flywheel," in *Signal and Information Processing, Networking and Computers: Proceedings of the 8th International Conference on Signal and Information Processing, Networking and Computers (ICSINC)*, pp. 655-663, 2022.

[30] A. Mahmoudi, W. L. Soong, and A. Chiba, "Guest Editorial Design and Optimisation of Electric Motors for Transport Electrification," *IEEE Transactions on Industry Applications*, vol. 59, no. 2, pp. 1240-1241, 2023.

[31] I. Suwarno, Y. Finayani, R. Rahim, J. Alhamid, and A. R. Al-Obaidi, "Controllability and observability analysis of DC motor system and a design of FLC-based speed control algorithm," *Journal of Robotics and Control (JRC)*, vol. 3, no. 2, pp. 227-235, 2022.

[32] S. W. Shneen, H. S. Dakheel, and Z. B. Abdullah, "Design and Implementation of No Load, Constant and Variable Load for DC Servo Motor," *Journal of Robotics and Control (JRC)*, vol. 4, no. 3, pp. 323-329, 2023.

[33] R. Alika, E. M. Mellouli, and E. H. Tissir, "Adaptive cruise control of the autonomous vehicle based on sliding mode controller using arduino and ultrasonic sensor," *Journal of Robotics and Control (JRC)*, vol. 5, no. 1, pp. 301-311, 2024.

[34] H. Budiarto, V. Triwidyaningrum, F. Umam, and A. Dafid, "Implementation of Automatic DC Motor Braking PID Control System on (Disc Brakes)," *Journal of Robotics and Control (JRC)*, vol. 4, no. 3, pp. 371-387, 2023.

[35] D. A. N. K. Suhermanto *et al*., "Monitoring DC Motor Based on LoRa and IOT," *Journal of Robotics and Control (JRC)*, vol. 5, no. 1, pp. 54-61, 2024.

[36] A. Wongkamhang *et al*., "Design and Develop a Non-Invasive Pulmonary Vibration Device for Secretion Drainage in Pediatric Patients with Pneumonia," *Journal of Robotics and Control (JRC)*, vol. 4, no. 5, pp. 632-642, 2023.

[37] M. Fazilat and N. Zioui, "The impact of simplifications of the dynamic model on the motion of a six-jointed industrial articulated robotic arm movement," *Journal of Robotics and Control (JRC)*, vol. 5, no. 1, pp. 173-186, 2024.

[38] R. D. Puriyanto and A. K. Mustofa, "Design and implementation of fuzzy logic for obstacle avoidance in differential drive mobile robot," *Journal of Robotics and Control (JRC)*, vol. 5, no. 1, pp. 132-141, 2024.

[39] M. Afkar, R. Gavagsaz-Ghoachani, M. Phattanasak, S. Pierfederici, and W. Saksiri, "Local-stability analysis of cascaded control for a switching power converter," *Journal of Robotics and Control (JRC)*, vol. 5, no. 1, pp. 160-172, 2024.

[40] M. A. Abdelghany, A. O. Elnady, and S. O. Ibrahim, "Optimum PID controller with fuzzy self-tuning for DC servo motor," *Journal of Robotics and Control (JRC)*, vol. 4, no. 4, pp. 500-508, 2023.

[41] D. A. Magallón, C. E. Castañeda, F. Jurado, and O. A. Morfin, "Design of a neural super-twisting controller to emulate a flywheel energy storage system," *Energies*, vol. 14, no. 19, p. 6416, 2021.

[42] Z. Zhang, X. Zhai, S. Cheng, Z. Wen, M. Yao, and Z. Yan, "Variable damping mechanism and verification of the torsional damper for a parallel-series hybrid electric vehicle," *Journal of Vibroengineering*, vol. 26, no. 8, pp. 1746-1762, 2024.

[43] A. L. Pogudin, E. A. Chabanov, A. D. Korotaev, D. A. Oparin, and P. V. Kuleshov, "Development of a Torsion Test Bench Electric Drive Based on Arc Induction Motors," *Russian Electrical Engineering*, vol. 93, no. 11, pp. 718-722, 2022.

[44] E. R. Gomez, J. Sjöstrand, L. Kari, and I. L. Arteaga, "Torsional vibrations in heavy-truck powertrains with flywheel attached centrifugal pendulum vibration absorbers," *Mechanism and Machine Theory*, vol. 167, pp. 104547, 2022.

[45] G. Paillot, S. Chesné, and D. Rémond, "Hybrid coupled damper for the mitigation of torsional vibrations and rotational irregularities in an automotive crankshaft: Concept and design subtleties," *Mechanics Based Design of Structures and Machines*, vol. 51, no. 6, pp. 3242-3259, 2023.

[46] K. Wu, Z. Liu, Q. Ding, F. Gu, and A. Ball, "Torsional vibration responses of the engine crankshaft-gearbox coupled system with misfire and breathing slant crack based on instantaneous angular speed," *Mechanical Systems and Signal Processing*, vol. 173, pp. 109052, 2022.

[47] B. Ruan and G. Wu, "Torsional vibration analysis and optimisation of a hybrid vehicle powertrain," *International Journal of Vehicle Performance*, vol. 9, no. 4, pp. 337-357, 2023.

[48] M. Wang, N. Xiao, and M. Fan, "The torsional vibration simulation of the diesel engine crankshaft system based on multi-body dynamic model," *Proceedings of the Institution of Mechanical Engineers, Part K: Journal of Multi-body Dynamics*, vol. 235, no. 3, pp. 443-451, 2021.

[49] Q. Han, S. Gao, and F. Chu, "Micro-Vibration Analysis, Suppression, and Isolation of Spacecraft Flywheel Rotor Systems: A Review," *Vibration*, vol. 7, no. 1, pp. 229-263, 2024.

[50] G. S. Nagali, N. Samanvita, V. Hegde, and R. Babu, "Design of flywheel energy generation system," *Intellectual Journal of Energy Harvesting and Storage*, vol. 2, no. 2, pp. 95-124, 2024.

[51] J. F. Kayode, B. A. Adaramola, J. O. Akinyoola, T. M. Azeez, S. A. Afolalu, and A. O. Akinola, "Modelling and Optimization of Torsional Stiffness of a Crankshaft," in *2024 International Conference on Science, Engineering and Business for Driving Sustainable Development Goals (SEB4SDG)*, pp. 1-9, 2024.

[52] Z. Yan, D. Yin, L. Chen, and W. Shen, "Research on the torsional vibration performance of a CVT powertrain with a dual-mass flywheel damper system," *Proceedings of the Institution of Mechanical Engineers, Part D: Journal of Automobile Engineering*, vol. 236, no. 6, pp. 1144-1154, 2022.

[53] V. G. Nair, "Efficient Path Planning Algorithm for Mobile Robots Performing Floor Cleaning Like Operations," *Journal of Robotics and Control (JRC)*, vol. 5, no. 1, pp. 287-300, 2024.

[54] D. Patel and K. Cohen, "Obstacle avoidance and target tracking by two wheeled differential drive mobile robot using ANFIS in static and dynamic environment," in *Fuzzy Information Processing 2020: Proceedings of the 2020 Annual Conference of the North American Fuzzy Information Processing Society, NAFIPS 2020*, pp. 337–348, 2022.

[55] I. A. Hassan, I. A. Abed, and W. A. Al-Hussaibi, "Path planning and trajectory tracking control for two-wheel mobile robot," *Journal of Robotics and Control (JRC)*, vol. 5, no. 1, pp. 1-15, 2024.

[56] N. M. Alyazidi, A. M. Hassanine, M. S. Mahmoud, and A. Ma'arif, "Enhanced Trajectory Tracking of 3D Overhead Crane Using Adaptive Sliding-Mode Control and Particle Swarm Optimization," *Journal of Robotics and Control (JRC)*, vol. 5, no. 1, pp. 253-262, 2024.

[57] E. Rijanto, N. Changgraini, R. P. Saputra, and Z. Abidin, "Key Factors that Negatively Affect Performance of Imitation Learning for Autonomous Driving," *Journal of Robotics and Control (JRC)*, vol. 5, no. 1, pp. 239-252, 2024.

[58] P. Chotikunnan, R. Chotikunnan, and P. Minyong, "Adaptive parallel iterative learning control with a time-varying sign gain approach empowered by expert system," *Journal of Robotics and Control (JRC)*, vol. 5, no. 1, pp. 72-81, 2024.

[59] E. Kurniawan *et al*., "A performance evaluation of repetitive and iterative learning algorithms for periodic tracking control of functional electrical stimulation system," *Journal of Robotics and Control (JRC)*, vol. 5, no. 1, pp. 205-216, 2024.

[60] M. Alzubi, M. Almseidin, S. Kovacs, J. Al-Sawwa, and M. Alkasassbeh, "EI-FRI: Extended incircle fuzzy rule interpolation for multidimensional antecedents, multiple fuzzy rules, and extrapolation using total weight measurement and shift ratio," *Journal of Robotics and Control (JRC)*, vol. 5, no. 1, pp. 217-227, 2024.

[61] O. Y. Ismael, M. Almaged, and A. I. Abdulla, "Nonlinear model predictive control-based collision avoidance for mobile robot," *Journal of Robotics and Control (JRC)*, vol. 5, no. 1, pp. 142-151, 2024.

[62] R. R. D. Maity, R. K. Mudi, and C. Dey, "Stable optimal self-tuning interval type-2 fuzzy controller for servo position control system," *International Journal of Automation and Control*, vol. 16, no. 5, pp. 594–620, 2022.

[63] O. Tachinina, O. Lysenko, I. Alekseeva, I. Sushyn, and V. Novikov, "Method of algorithmic correction of dynamic properties of special-purpose electric drive," in *2022 IEEE 3rd KhPI Week on Advanced Technology (KhPIWeek)*, pp. 1-4, 2022.

[64] M. M. Rashid and S. M. Salam, "Controlling the Variable Inertia of Flywheel: A Scientific Review," *Asian Journal of Electrical and Electronic Engineering*, vol. 4, no. 1, pp. 17-28, 2024.

[65] Z. Yao, T. Lin, H. Ren, and S. Fu, "Electromechanical coupling dynamic responses of motor-gear system under different motor control methods," *Journal of Low Frequency Noise, Vibration and Active Control*, p. 14613484241299469, 2024.

[66] P. Bucha, L. Rolník, J. Lovíšková, and M. Naď, "Modification of rotor modal properties based on structural changes in the stiffness of its bearings and shaft," in *Journal of Physics: Conference Series*, vol. 2712, no. 1, p. 012022, 2024.

[67] V. S. Nemagoud and K. K. Dutta, "Effective Torque Ripple Reduction of Permanent Magnet Brushless DC Motor," *International Journal of Electronics Signals and Systems*, pp. 131–136, 2022.

[68] V. P. Sharma, V. P. Meena, V. P. Singh, K. Murari, and A. Mathur, "Reduction of Interconnected Hybrid Power System Using Direct Truncation and Routh Array Method," in *2023 IEEE International Conference on Energy Technologies for Future Grids (ETFG)*, pp. 1-6, 2023.

[69] L. H. Zhang and R. C. Li, "Quality of Approximate Balanced Truncation," *arXiv preprint arXiv:2406.05665*, 2024.

[70] P. Andreou, S. Theodossiades, A. Z. Hajjaj, M. Mohammadpour, and M. R. Souza. *Reduced Order Model for Modal Analysis of Electric Motors Considering Material and Dimensional Variations*. SAE Technical Paper, 2024.

[71] H. Yadavari, V. T. Aghaei, and S. I. GLU, "Addressing challenges in dynamic modeling of stewart platform using reinforcement learning-based control approach," *Journal of Robotics and Control (JRC)*, vol. 5, no. 1, pp. 117-131, 2024.

[72] M. Zhang, S. Bai, A. Xia, W. Tuo, and Y. Lv, "Reduced Order Modeling of System by Dynamic Modal Decom-Position with Fractal Dimension Feature Embedding," *Fractal and Fractional*, vol. 8, no. 6, p. 331, 2024.

[73] L. Moin and V. Uddin, "Application of Tree Structured Transfer Function to an electromechanical system, its Comparison with Conventional Method and Application for Order Reduction," in *International Conference on Computational Intelligence for Modelling, Control and Automation and International Conference on Intelligent Agents, Web Technologies and Internet Commerce (CIMCA-IAWTIC'06)*, vol. 2, pp. 562-567, 2005.

[74] G. Chen, Y. Cao, D. Qing, and Y. Wang, "Truncation error correction by designing input-adjustment-output coefficients for dynamic matrix control based on cubic spline function," *Simulation*, vol. 100, no. 8, pp. 813-822, 2024.

[75] H. Kang, Q. Yuan, X. Su, T. Guo, and Y. Cong, "Modal truncation method for continuum structures based on matrix norm: modal perturbation method," *Nonlinear Dynamics*, vol. 112, no. 13, pp. 11313-11328, 2024.

[76] S. Sun, B. Yang, Q. Zhang, R. Wüchner, L. Pan, and H. Zhu, "Long-term continuous automatic modal tracking algorithm based on Bayesian inference," *Structural Health Monitoring*, vol. 23, no. 3, pp. 1530-1546, 2024.

[77] R. K. Németh and B. B. Geleji, "Modal truncation damping in reduced modal analysis of piecewise linear continuum structures," *Mechanics Based Design of Structures and Machines*, vol. 51, no. 3, pp. 1582–1605, 2023.

[78] A. C. Dederichs and O. Øiseth, "A novel and near-automatic mode tracking algorithm for civil infrastructure," *Journal of Sound and Vibration*, vol. 573, p. 118217, 2024.

[79] J. Hewitt, C. D. Manning, and P. Liang, "Truncation sampling as language model desmoothing," *arXiv preprint arXiv:2210.15191*, 2022.

[80] M. Tarpø, M. Vigsø, and R. Brincker, "Modal truncation in experimental modal analysis," in *Topics in Modal Analysis & Testing, Volume 9: Proceedings of the 36th IMAC, A Conference and Exposition on Structural Dynamics 2018*, pp. 143-152, 2018.